ORIGINAL ARTICLE

Concordance in phylogeography and ecological niche modelling identify dispersal corridors for reptiles in arid Australia

Jane Melville[1]*, Margaret L. Haines[1], Joshua Hale[1], Stephanie Chapple[1] and Euan G. Ritchie[2]

[1]*Department of Sciences, Museum Victoria, Melbourne, Victoria 3001, Australia,* [2]*Deakin University, Geelong, Australia, School of Life and Environmental Sciences, Centre for Integrative Ecology (Burwood Campus), 221 Burwood Highway, Burwood, Victoria 3125, Australia*

ABSTRACT

Aim Using the rock-specialist agamid *Ctenophorus caudicinctus* as a model, we test hypothesized biogeographical dispersal corridors for lizards in the Australian arid zone (across the western sand deserts), and assess how these dispersal routes have shaped phylogeographical structuring.

Location Arid and semi-arid Australia.

Methods We sequenced a *c.* 1400 bp fragment of mtDNA (*ND2*) for 134 individuals of *C. caudicinctus* as well as a subset of each of the mtDNA clades for five nuclear loci (*BDNF*, *BACH1*, *GAPD*, *NTF3*, and *PRLR*). We used phylogenetic methods to assess biogeographical patterns within *C. caudicinctus*, including relaxed molecular clock analyses to estimate divergence times. Ecological niche modelling (Maxent) was employed to estimate the current distribution of suitable climatic envelopes for each lineage.

Results Phylogenetic analyses identified two deeply divergent mtDNA clades within *C. caudicinctus* – an eastern and western clade – separated by the Western Australian sand deserts. However, divergences pre-date the Pleistocene sand deserts. Phylogenetic analyses of the nuclear DNA data sets generally support major mtDNA clades, suggesting past connections between the western *C. c. caudicinctus* populations in far eastern Pilbara (EP) and the lineages to the east of the sand deserts. Ecological niche modelling supports the continued suitability of climatic conditions between the Central Ranges and the far EP for *C. c. graafi*.

Main conclusions Estimates of lineage ages provide evidence of divergence between eastern and western clades during the Miocene with subsequent secondary contact during the Pliocene. Our results suggest that this secondary contact occurred via dispersal between the Central Ranges and the far EP, rather than the more southerly Giles Corridor. These events precede the origins of the western sand deserts and divergence patterns instead appear associated with Miocene and Pliocene climate change.

Keywords

Agamidae, Australia, *Ctenophorus caudicinctus*, desert lizards, dispersal corridors, phylogeography

*Correspondence: Jane Melville, Department of Sciences, Museum Victoria, GPO Box 666, Melbourne, Vic. 3001, Australia.
E-mail: jmelv@museum.vic.gov.au*

INTRODUCTION

The distribution of related lineages across a landscape and evidence of historical gene flow between them provide valuable insight into the process of divergence and ultimately speciation (Milá *et al.*, 2013). Phylogeographical studies at a large spatial scale and which encompass major geographical barriers to gene flow, as well as regions of secondary contact, are of particular interest because they can shed light on historical factors driving divergence. The Australian arid zone provides an ideal system to study the role of geographical barriers in intraspecific diversification at a large spatial scale,

over long time periods. Unlike regions in the Northern Hemisphere that have complex glaciation histories and significant topographic barriers to dispersal, Australia has had a relatively stable climate, largely without glaciation during the Pleistocene, and 'mountainous' regions are more subdued (Byrne *et al.*, 2008). The Australian arid zone is immense, consisting of *c.* 5.25 million km^2 covering almost 70% of the landmass (Byrne *et al.*, 2008). Although the Australian continent is relatively flat compared with other continents, the arid zone has a number of desert ranges (elevation < 1500 m) in central, western and northern regions (Fig. 1), constituting prominent topographic features that rise above the surrounding lowlands. These lowland regions in the western deserts, in particular, are dominated by sand plains and dune fields that have isolated the desert ranges with vast tracts of sandy soils. Thus, the mosaic of rocky and sandy habitats in Australia's arid zone has the potential to play an important role in diversification patterns and ultimately speciation in desert fauna.

Pianka (1972) developed a simple model to explain extensive speciation of lizards within the Australian deserts based on the spatial and temporal fluctuation of habitats, hypothesizing that the arid zone was comprised of a complex array of spatially differentiated habitats. As part of his model, Pianka (1972) identified Pleistocene dispersal routes across the western deserts, with the Giles Corridor extending across the central portion of the western sand deserts (Fig. 1). Although the late Miocene saw an increase in the aridity in this region but the spread of sand deserts in Western Australia occurred during the Pleistocene (Hill, 1994; Byrne *et al.*, 2008). Pianka (1972) suggested that the Giles Corridor functioned as an intermittent Pleistocene dispersal route between eastern and western arid-zone fauna and remains the only proposed dispersal route for reptiles in the region. It is a continuous band of *Acacia* shrublands linking the east Murchison goldfields in Western Australia to the Central Ranges by extending through the Lake Carnegie region in the Great Victoria Desert and the southern part of the Gibson Desert (Van Oosterzee, 1991). A number of recent studies have tested Pianka's (1972) hypotheses using phylogenetic and phylogeographical approaches, with the prediction that arid-zone lizards should exhibit phylogeographical structuring concordant with the distribution of the major vegetation communities in central Australia (e.g. Chapple *et al.*, 2004; Shoo *et al.*, 2008; Pepper *et al.*, 2011a,b). Results from these studies are mixed, where a study on *Egernia* skinks failed to provide strong support for ecological and habitat factors being responsible for the diversification (Chapple *et al.*, 2004), while Shoo *et al.* (2008) found strong genetic divergence between habitat patches in pebble-mimic dragon lizards. Pepper *et al.* (2011a) found that geological, landscape and climate evolution have played an important role in the diversification of saxicolous and desert lineages of *Heteronotia* geckos. However, these studies have found no genetic evidence supporting historical dispersal routes

across the western deserts, instead both studies of rock specialists found deeply divergent lineages on either side of the sand deserts, with no evidence of secondary contact (Shoo *et al.*, 2008; Pepper *et al.*, 2011a,b).

Ctenophorus caudicinctus (Günther 1875) provides an ideal opportunity to further investigate the relationship between habitat distributions, dispersal routes and diversification in Australia's western deserts. *Ctenophorus caudicinctus* is a rock-dwelling species that occurs in the western half of Australia (Fig. 1). It consists of six subspecies, distinguished on male morphology and colour patterns (Storr, 1967): *C. c. caudicinctus*, *C. c. mensarum*, *C. c. infans*, *C. c. macropus*, *C. c. slateri* and *C. c. graafi*. Despite the morphological distinctiveness of the subspecies, Storr (1967) was unable to assign all specimens examined to particular subspecies, particularly in contact zones between *C. c. caudicinctus*, *C. c. mensarum* and *C. c. infans*. Additionally, populations from the northern extent of the range were left unidentified, with the exception of the description of *C. c. macropus* from western Arnhem Land. In a later publication the distribution of *C. c. macropus* was extended to incorporate these formerly unidentified northern populations from the Kimberley in Western Australia across to north-western Queensland (Storr *et al.*, 1983). As these morphological studies there has been very little research conducted on *Ctenophorus caudicinctus*, although more recent molecular work has indicated that it is closely related to the rock-dwelling species *C. ornatus* from south-western Western Australia (Melville *et al.*, 2001; Schulte *et al.*, 2003).

We investigate dispersal routes and diversification in Australia's western deserts in a comprehensive phylogeographical study of *Ctenophorus caudicinctus*, incorporating six genes and ecological niche modelling (ENM), to examine the relative importance of habitat distributions. We focus, in particular, on the Great Sandy Desert, the Gibson Desert and Great Victoria Deserts, testing the hypothesis that the Giles Corridor provides a dispersal route across the western sand deserts. Based on the distributions of subspecies, we would expect evidence of gene exchange between *C. c. mensarum* and *C. c. graafi* if the Giles Corridor has provided a dispersal route through the sand deserts (Fig. 1). We predicted that the Giles Corridor – a band of *Acacia* shrublands – would not make an obvious dispersal corridor for a rock-specialist species, such as *C. caudicinctus*. We employ relaxed molecular clock analyses to estimate divergence times within *C. caudicinctus* in order to determine whether phylogeographical patterns are consistent with the Giles Corridor being a Pleistocene dispersal route in this species. We also use ENM to determine if suitable climatic conditions currently exist for dispersal of *C. caudicinctus* across the western deserts. ENM has been successfully incorporated into phylogeographical studies to address such concepts. GIS-based models predicting the geographical distribution of sister species have provided a valuable method of investigating the role of ecological factors in driving diversification (Kozak *et al.*, 2008).
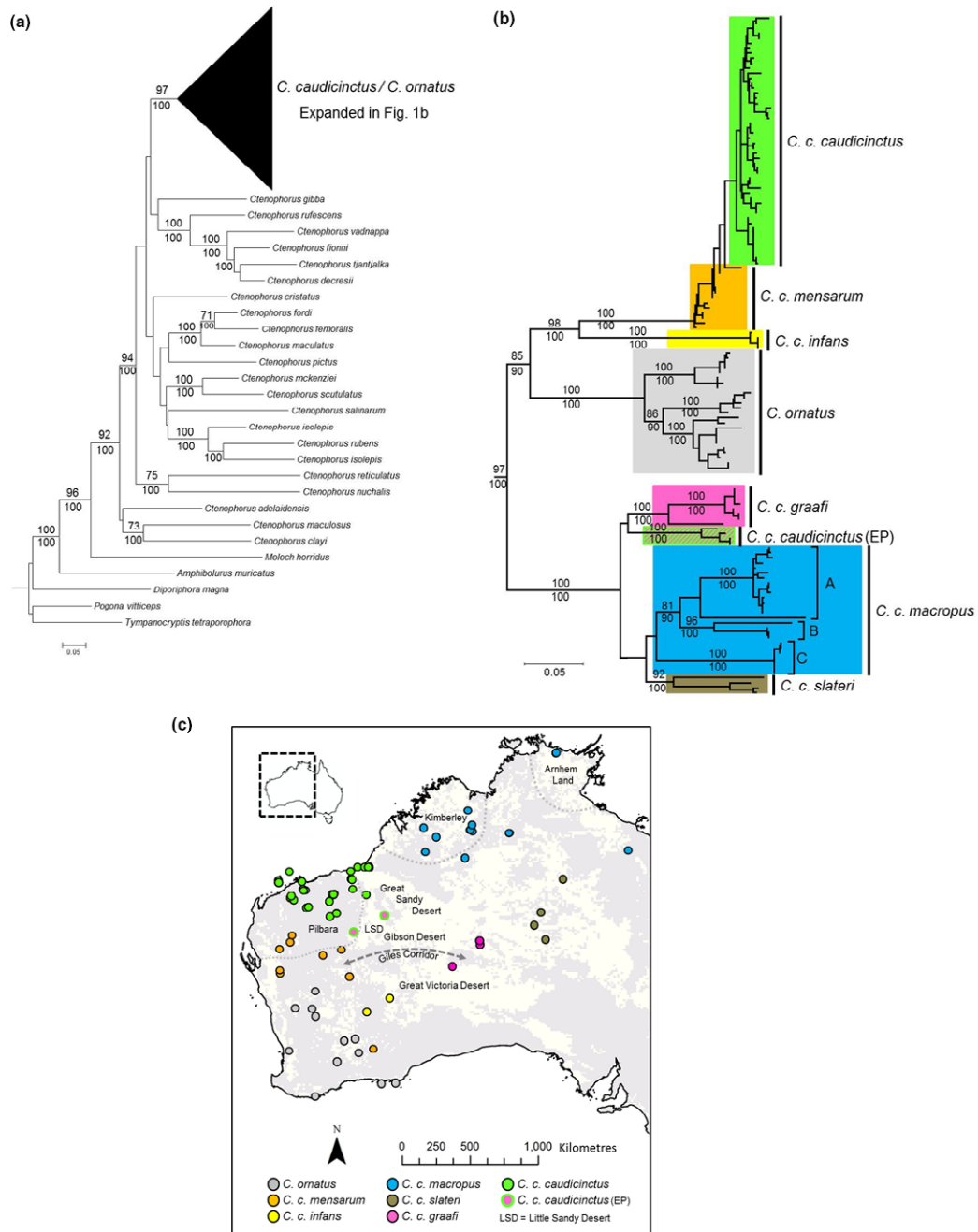
Figure 1 Maximum likelihood phylogenetic tree for *Ctenophorus ornatus* and the six subspecies of *C. caudicinctus* based on *c.* 1400 bp mitochondrial DNA (*ND2*). Samples sequenced in this study and previously published sequences are designated by tissue or museum registration numbers and GenBank numbers (see Appendix S1 for details). ML bootstraps > 70% (above) and Bayesian posterior probabilities > 90% (below) are provided on branches. Colours designate clades, which are mapped – pale yellow shading on the locality map indicates the distribution of sand deserts and major desert systems, the Giles Coridor and other biogeographical features have been labelled.

MATERIALS AND METHODS

Tissue samples

We collected specimens of *Ctenophorus caudicinctus* and associated tissues for sequencing with two main objectives. First, we endeavoured to maximize geographical spread and second we sought to fill in geographical gaps in tissue samples already held in Australian museums. Thirty-eight field-collected tissue samples of *C. caudicinctus* were included in the study (see Appendix S1 in Supporting Information). An additional 96 tissue samples of *C. caudicinctus* and *C. ornatus* were obtained from museum collections (see Appendix S1). These museum samples combined with the field-collected tis-

sues provided comprehensive sampling for the study species. We also included previously published sequences as outgroups for our analyses and sequenced additional outgroup species, where required.

Laboratory protocols and alignment of DNA sequences

Genomic DNA was extracted from tail tips or liver samples using a DNeasy Blood and Tissue Kit (Qiagen, Germantown, MD, USA) as per manufacturer's instructions or using a using Proteinase K digestion and chloroform-isoamyl alcohol extraction. For all specimens, a fragment (c. 1400 bp) of the mtDNA genome was amplified that includes *ND2* and flanking tRNAs (see Melville et al., 2011 for primer sequences and protocols). For a subset of specimens, we sequenced five nuclear loci (*BDNF*, *BACH1*, *GAPD*, *NTF3*, and *PRLR*). In previous phylogeographical studies of Australian agamids it has been common to use the nuclear exon RAG1, however, previous work on *C. caudicinctus* and *C. ornatus* found that there is significant intraspecific length variation in the N-terminal domain of this gene in these species (Melville & Hale, 2009), thus, this regions was not included in our study. Oligonucleotide primer pairs for the mitochondrial and five nuclear genes are listed in Appendix S2.

Amplifications for *ND2* and *BDNF* were performed in 25 μL volumes in the presence of 1.5 mM MgCl$_2$, 0.2 mM dNTPs, 0.2 μM of forward and reverse primer, 1x Qiagen polymerase chain reaction (PCR) buffer and 1 U of HotStarTaq DNA polymerase (Qiagen). For *BACH1*, *GAPD*, *NTF3* and *PRLR*, amplifications were performed in 20 μL volumes in the presence of 0.25 μM of forward and reverse primer and 50 U of GoTaq Hot Start (Promega, Madison, WI, USA). PCR protocols for mitochondrial and nuclear genes are listed in Appendix S2. PCR amplifications were visualized on a 1.2% agarose mini-gel and amplified products were purified using either GFX spin columns, using SureClean Plus (BIOLINE, London, UK), or ExoSAP-IT (Affymetrix, Santa Clara, CA, USA). Purified product was sent to Macrogen (Korea) for sequencing. Sequence chromatograms were edited using Geneious 6.1.8 (Biomatters Ltd, Auckland, New Zealand) to produce a single continuous sequence for each specimen. Mitochondrial DNA sequences were aligned using tRNA secondary structure models (Macey et al., 1997), and protein-coding regions were translated to amino acids to check alignment and for stop codons.

Phylogenetic analyses

Phylogenetic analysis of all samples for the mtDNA gene region was undertaken using maximum likelihood and Bayesian analyses. Published *ND2* sequences of 22 other *Ctenophorus* species, plus five species from other Australian agamid genera were included in analyses as outgroups. To investigate phylogenetic relationships between the *C. caudicinctus* subspecies, 134 new sequences and 28 previously published sequences were analysed for the *ND2* protein-coding gene. The alignment comprised 1425 characters: 865 characters were variable and 721 characters were parsimony informative. Maximum likelihood phylogenetic trees were estimated using PhylML 2.1.0 (Guindon & Gascuel, 2003) implemented in Geneious 6.1.2 (Biomatters Ltd), using a BEST topology search. Analyses were performed using a GTR+I+Γ model, estimated using MrModeltest 2.3 with the Akaike information criterion: γ = 0.7936; proportion of invariable sites = 0.2805; substitution rates A↔C 0.5529, A↔G 7.3567, A↔T 0.6780, C↔G 0.2001, C↔T 4.5134, G↔T 1.0000; and, nucleotide frequencies A = 0.4054, C = 0.3199, G = 0.0747 and T = 0.2000. Bootstrap resampling (Felsenstein, 1985) was applied to assess support for individual nodes in each above-mentioned analysis using 100 bootstrap replicates in PhylML with the same settings as above.

Bayesian analyses were performed in MrBayes 3.2 (Ronquist et al., 2012) using the evolutionary model selected by MrModeltest 2.3 with parameters estimated from data during the analysis. Four Markov chains were used in each of two simultaneous runs starting from different random trees. Analyses were run for 10 million generations for each data set. Standard deviation of split frequencies was used as a convergence diagnostic to confirm suitability of run length. For all analyses, it was confirmed that potential scale reduction factor values were close to 1.0, indicating that an adequate sample of the posterior probability distribution had been achieved (Ronquist et al., 2012). In addition, the output was examined using Tracer 1.5 (Rambaut & Drummond, 2003) to check that stationarity had been reached. Bayesian analyses for *BDNF*, *BACH1*, *GAPD*, *NTF3*, and *PRLR* were repeated for the subset samples, consisting of 68 ingroup and four outgroup samples. Identical run conditions to the *ND2* analyses were used for these analyses, except for the models of evolution implemented (Table 1). Models of sequence evolution were selected using MrModeltest 2.3.

Table 1 Details of sequence length, number of parsimony informative characters models of evolution, Mr Bayes settings and mean log likelihood of the Bayesian tree for each of the nuclear gene regions.

Gene region	Length (bp)	Number of sequences	Number of parsimony informative characters	Model of evolution	Log likelihood (−ln)
BACH1	1030	68	63	GTR+I+Γ	−2745.76
BDNF	841	68	26	GTR+I	−1783.73
PRLR	512	66	55	GTR+I+Γ	−1939.35
NTF3	610	68	20	HKY+I	−1243.57
GAPD	253	65	23	HKY+Γ	−821.98

We used a Bayesian framework for subspecies tree estimation, incorporating all gene regions (*ND2*, *BDNF*, *BACH1*, *GAPD*, *NTF3* and *PRLR*), to determine phylogenetic relationships between subspecies across the six gene regions. We used a reduced *ND2* data set, matching sequence data for individuals in the nuclear DNA data set, resulting in six data sets of 72 individuals. Populations of *C.c. caudicinctus* from the eastern Pilbara (EP), which aligned with *C. graafi* in the mtDNA data set, was coded as a stand-alone group for the species tree analysis, while all other samples were coded according to their subspecies designation. We used *BEAST, enabled in BEAST 1.7.5, to co-estimate the six gene trees embedded in a shared species tree (see Heled & Drummond, 2010). Unlinked substitutions models were employed across the loci, based on preliminary analyses using MRMODELTEST 2.3 (Table 1). A Yule process species tree prior was specified and the gene tree priors were automatically specified by the multispecies coalescent. The analysis was run for 50 million generations. The output was examined using TRACER 1.5 (Rambaut & Drummond, 2003) to check that stationarity had been reached.

Divergence times estimates

A relaxed molecular clock method within the program BEAST 1.7.5 was used to estimate divergence times for each of the *C. caudicinctus* subspecies, based on the mtDNA data set. Additional published sequences were used in the analysis to allow placement of calibration points, as detailed in Melville *et al.* (2011). We used lognormally distributed fossil calibrations, including four *Iguania* fossils detailed in previous studies (see Melville *et al.*, 2011): a middle Jurassic acrodont iguanian fossil (154–180 Ma), an early Miocene sceloporine (22.8 Ma), a *Chamaeleo/Rhampholeon* fossil (18 Ma) and a Pliocene *Phrynocephalus* fossil (5 Ma). Specific BEAST settings for these calibrations are as per table 3 in Melville *et al.* (2011). In addition, we added a minimum age estimate for the ingroup of Australian amphibolurine species, with a fossil of the *Physignathus lesueurii* lineage, of 20 Ma (Covacevich *et al.*, 1990) with BEAST settings detailed in Edwards & Melville (2011). The analysis was run for 20 million generations using a GTR+I+Γ model of evolution with a Speciation: Yule Process tree prior and a random starting tree. The output was examined using TRACER 1.5 (Rambaut & Drummond, 2003) to check that stationarity had been reached and to assess the autocorrelation of rates from ancestral to descendant lineages, as detailed in the results (Drummond *et al.*, 2006).

Ecological niche modelling

We used the environmental niche modelling algorithm MAXENT 3.3.3 (Elith *et al.*, 2011), with default settings, to create predicted current distributions (climate envelopes) for each of the *Ctenophorus* subspecies, except for *C. c. infans*, which was omitted due to insufficient records. Locality records for all subspecies were collected from across their distributions by E.G.R. and J.M. and supplemented with further records from additional museum databases (see Acknowledgements). Reliability of all records was assessed with reference to current known distributions and according to our own and expert knowledge of each subspecies; dubious records were excluded from the final data set. To reduce problems of over-fitting and co-linearity of variables in our models, we used eight climatic variables (annual mean temperature, temperature seasonality, maximum temperature of the warmest month, minimum temperature of the coldest month, annual precipitation, precipitation seasonality, precipitation of the wettest quarter and precipitation of the driest quarter, as per McMahon *et al.* (1995) and a soil layer (categorized as sand or other substratum, modified from Fordham *et al.*, 2012). We chose these variables as they are known to be important in influencing the distributions of vertebrates, including reptiles, across our study region (Ritchie *et al.*, 2008; Melville *et al.*, 2011).

RESULTS

Phylogenetic relationships

Mitochondrial DNA

The mtDNA Bayesian and ML trees (Fig. 1) recovered two monophyletic lineages within the *C. caudicinctus* and *C. ornatus* group. These lineages represent a western and eastern clade, with the western clade comprising *C. ornatus, C. c. infans, C. c. mensarum* and *C. c. caudicinctus*. The monophyly of this western lineage only received moderate support (85% bootstrap; 90% posterior probability), with *C. ornatus* being the basal group; however, the monophyly of all the western *C. caudicinctus* subspecies was highly supported (98% bootstrap; 100% posterior probability). Within the western *C. caudicinctus* subspecies, the *C. c. infans* clade received high support (100% bootstrap; 100% posterior probability), while *C. c. caudicinctus* and *C. c. mensarum* were not supported as being independent evolutionary lineages, although all the *C. c. mensarum* samples formed the basal lineages in a clade containing *C. c. caudicinctus* and *C. c. mensarum*. These two subspecies were highly supported as a single monophyletic lineage (100% bootstrap; 100% posterior probability).

The eastern clade received strong support (100% bootstrap; 100% posterior probability), with the monophyly of both *C. c. graafi* (100% bootstrap; 100% posterior probability) and *C. c. slateri* being well supported (92% bootstrap; 100% posterior probability). *C. c. macropus* was not supported as monophyletic but instead contained three well supported lineages: A. Western Australia and western Northern Territory; B. Arnhem Land; and C. western Queensland. One sample of *C. c. macropus* from the south-western Kimberley was highly diverged from the remainder of the Kimberley samples. Additionally, there were four samples of *C. c. caudicinctus* from the far eastern Pilbara area (designated as 'EP' hence forth) that fell within the eastern phylogenetic clade, as the sister lineage to *C. c. graafi,* although this relationship was not well supported.

Examination of mean uncorrected *P* distance of mtDNA between subspecies (Table 2) indicates deep divergences between all subspecies (8.97–14.88%), a level often seen between species, indicating a long history of vicariance. The exception to these deep divergences is the low level of mean uncorrected p distance of mtDNA between *C. c. caudicinctus* and *C. c. mensarum* (1.97%). In addition, the far EP *C. c. caudicinctus* populations that fall within the eastern clade phylogenetically are also deeply diverged from all other *C. caudicinctus* subspecies (8.08–15.04%).

Nuclear DNA

A subset of *C. caudicinctus* and *C. ornatus* samples were sequenced for *BDNF*, *BACH1*, *GAPD*, *NTF3*, and *PRLR*, ensuring all mtDNA lineages were represented. Sequence length, number of phylogenetically informative sites and models of evolution implemented in Bayesian analyses for each gene region are provided in Table 1. All nuclear data sets were complete, except for *GAPD*, which was missing three sequences (NMVD73949, SAMAR91440, WAMR131013), and PRLR, which was missing two ingroup sequences (WAMR139051, NMVD74380) and one outgroup (*C. adelaidensis*). Although there was less resolution of phylogenetic relationships in the nuclear regions, compared with the mtDNA tree, a number of consistent patterns were present across the gene regions. The Bayesian trees (see Appendix S3) for each of the five nuclear genes recovered mtDNA monophyletic lineages of *C. c. infans* and *C. ornatus*. In three genes (BDNF, GAPD, NTF3) *C. c. graafi* and *C. c. caudicinctus* (EP) were recovered as an monophyletic lineage. In the *BACH1* Bayesian tree, both *C. c. graafi* and *C. c. caudicinctus* (EP) were resolved as being in the eastern lineage including, *C.c. slateri* and *C. c. macropus*. Similarly, in *PRLR*, *C. c. graafi* and one of the *C. c. caudicinctus* (EP) samples (WAMR102635) were resolved as being in a clade containing the eastern lineages (*C. c. slateri* and *C. c. macropus*), while the two remaining *C. c. caudicinctus* (EP) samples (WAMR102611, WAMR102084) fell outside this clade in a

Table 2 Mean uncorrected mtDNA sequence divergence between subspecies of *Ctenophorus caudicinctus* and *C. ornatus*. Values given are percentages.

	1	2	3	4	5	6	7
1. *C. c. macropus*							
2. *C. c. slateri*	8.97						
3. *C.c. infans*	14.74	14.86					
4. *C. c. graafi*	9.09	9.36	14.88				
5. *C. c. caudicinctus*	14.28	14.48	11.33	13.95			
6. *C. c. caudicinctus* (EP)	8.90	8.67	15.04	8.08	13.68		
7. *C. c. mensarum*	13.88	14.14	11.15	13.71	1.97	13.33	
8. *C. ornatus*	14.25	13.95	13.38	14.07	13.04	13.26	12.96

number of samples for which phylogenetic relationships were unresolved.

Subspecies tree estimation

A reduced *ND2* data set, matching sequence data for individuals in the nuclear data sets, was used, resulting in two data sets of 72 individuals. A new MrModelTest analysis was conducted on this reduced mtDNA data set to estimate the optimal model of evolution, with a GTR+I+Γ model selected and implemented in the species tree analysis. The posterior parameter value estimates from the *beast species tree analysis were characterized by high (> 200) effective sample sizes and convergence of the individual runs was confirmed from assessments using Tracer. The maximum clade credibility trees from the posterior sets of species trees differed between each gene (Fig. 2). The topology of the mtDNA and nuclear trees were similar to that in the Bayesian analyses, although the nuclear trees show a higher level of resolution. The monophyly of *C. ornatus* and *C. c. infans* was highly supported across all gene regions. In all genes, except *PRLR*, *C. c. graafi* and *C. c. caudicinctus* (EP) are resolved as being sister lineages. In the *PRLR* tree, as in the Bayesian tree, *C. c. graafi* and one of the *C. c. caudicinctus* (EP) samples (WAMR102635) were resolved as being in a clade containing the eastern lineages (*C. c. slateri* and *C. c. macropus*); however, in this analysis the two remaining *C. c. caudicinctus* (EP) samples (WAMR102611, WAMR102084) were resolved as being part of the lineage containing *C. c. caudicinctus* and *C. c. mensarum*. In the *ND2* and *BACH1* trees *C. c. graafi* and the *C. c. caudicinctus* (EP) samples, were part of the eastern lineage with *C. c. slateri* and *C.c. macropus*, while in the *BDNF* and *GAPD* trees *C. c. graafi* and the *C. c. caudicinctus* (EP) samples, were part of the western lineage with *C. c. caudicinctus* and *C. c. mensarum*. In the overall species tree, *C. ornatus* and *C. c. infans* were highly supported as basal lineages in the complex. There was strong support for a western clade containing *C. c. caudicinctus* and *C.c. mensarum* in the overall species tree, although the *C. c. caudicinctus* (EP) samples were strongly supported as belonging to the eastern clade. The highly supported eastern clade containted *C. c. slateri*, *C. c. macropus*, *C. c. graafi* and the *C. c. caudicinctus* (EP) samples. Within this eastern clade *C. c. graafi* and the *C. c. caudicinctus* (EP) samples are highly supported as sister lineages, as are *C. c. slateri* and *C. c. macropus*.

Divergence times

The relaxed lognormal clock analysis of the mtDNA data set produced the same ingroup topology as the Bayesian and ML phylogenetic analyses (Fig. 1). Examination of the log file in Tracer 1.3 indicated a slight tendency towards a negative correlation in the rate of ancestral to descendant branches but zero was included in the 95% HPD (covariance: −0.0522; 95% credibility interval −0.3301 to 0.2478); thus, this autocorrelation was not considered significant (Drummond et al., 2006). The coefficient of rate variation
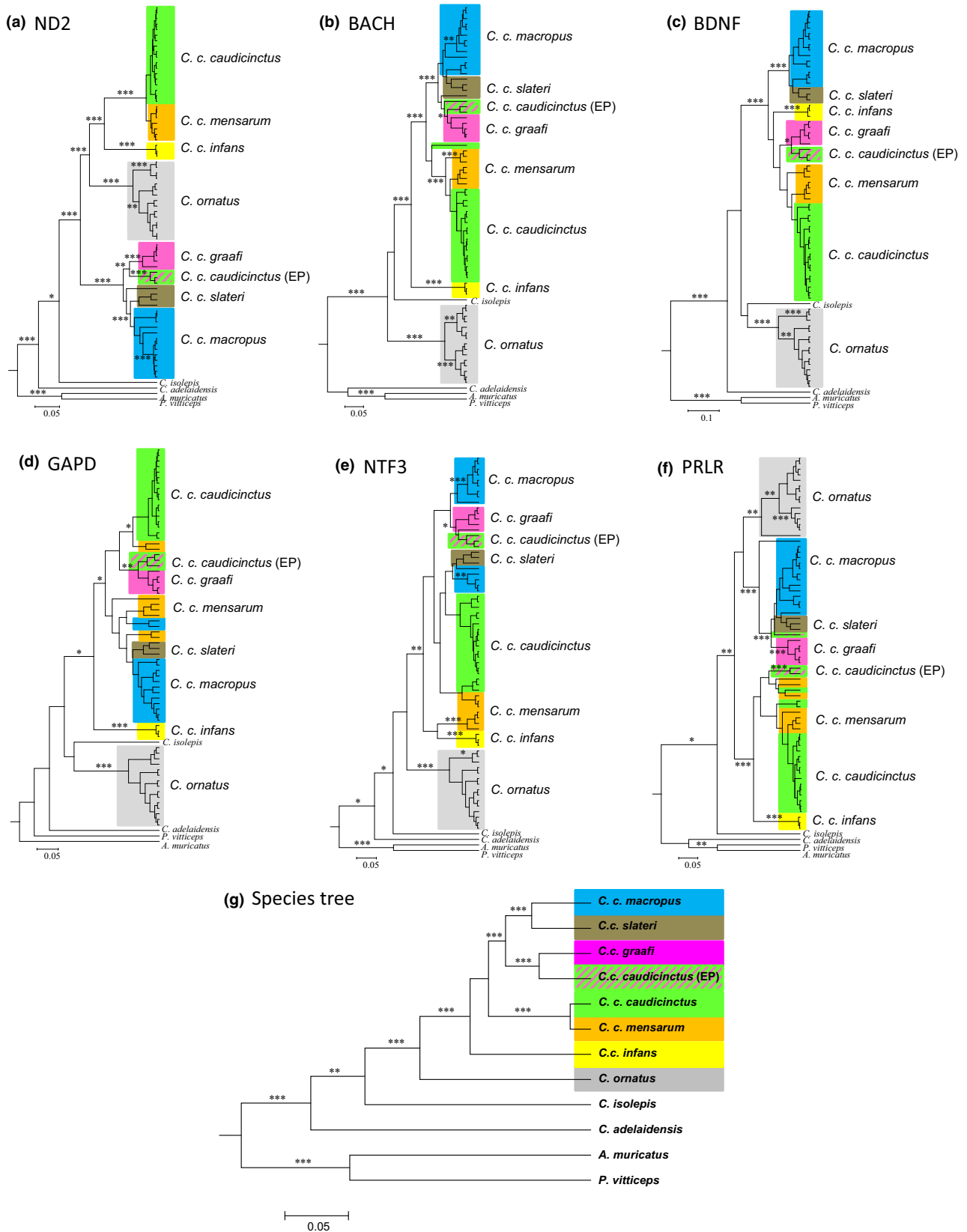
Figure 2 Gene and species tree phylogenies based on data sets inferred using ∗BEAST for the mtDNA and five nuclear genes (*BDNF*, *BACH1*, *GAPD*, *NTF3* and *PRLR*). Clade posterior probabilities are indicated on branches: ***> 98%; **90–97%; *80–89%. Colours designate clades mapped in Fig. 1.

was estimated to be 0.3374 (95% credibility interval 0.2096–0.4847), indicating that the dataset is not strictly clock-like and that a lognormal relaxed clock is appropriate. Age estimates (Table 3) indicate a mid-Miocene origin of the common ancestor of *C. caudicinctus* and *C. ornatus*. The *C. caudicinctus* lineages, both eastern and western, were estimated to be of late Miocene origins, as were each of the subspecies clades. An exception to this was the age of the common ancestor of *C. c. mensarum* and *C. c. caudicinctus*, which was much younger and probably Pleistocene in origin. In contrast, *C. c. graafi* and the *C. c. caudicinctus* populations from the far EP, which were grouped phylogenetically within the eastern *C. caudicinctus* mtDNA clade (Fig. 1), were estimated to have diverged in the Pliocene.

Ecological niche modelling

Overall our distribution models had very high predictive power, with an average area under curve of 0.98 (range 0.97–0.99). *Ctenophorus c. caudicinctus*'s climate envelope was restricted to the Pilbara region and *C. c. mensarum*'s climate envelope to the Southern Pilbara, Gascoyne and MidWest regions (Fig. 3). *Ctenophorus c. graafi*'s climate envelope, predominantly Central Australian, also spanned an area between *C. c. slateri* (Central Australia) and *C. c. caudicinctus*. *Ctenophorus c. macropus*'s distribution differed from all other subspecies (arid distributions) in being restricted to the monsoonal region of Northern Australia.

DISCUSSION

Dispersal routes through the western sand deserts

Previous phylogeographical studies have examined how the distributions of sand deserts in arid Australia have shaped

Table 3 Estimated age of the common ancestor of *Ctenophorus caudicinctus* and *C. ornatus* clades in millions of years, using relaxed molecular clock analyses, and mean estimate and 95% credibility intervals are provided based on mtDNA (ND2).

	Age of common ancestor (Ma)	95% credibility interval
C. ornatus and *C. caudicinctus*	9.4	7.1–12.1
Western *C. caudicinctus*: *C. c. infans*, *C. c. mensarum*, *C. c. caudicinctus*	5.5	3.4–7.6
Eastern *C. caudicinctus*: *C. c. macropus*, *C. c. slateri*, *C. c. graafi*, *C. c. caudicinctus* (EP)	5.3	3.7–7.2
C. c. mensarum and *C. c. caudicinctus*	0.9	0.4–1.7
C. c. macropus and *C. c. slateri*	5.0	3.5–6.7
C. c. graafi and *C. c. caudicinctus* (EP)	4.2	2.0–4.9

the evolutionary history and diversity of lizard species. Each of the studies investigating rock-dwelling lizards have found that the divergence of clades pre-dates the sand deserts and that geographically isolated species form deeply divergent and highly supported monophyletic lineages (e.g. Shoo et al., 2008; Pepper et al., 2011a). Shoo et al. (2008) and Chapple et al. (2004) had sought to test the role of dispersal routes through the sand deserts in shaping the biogeographical history of lizard species, but again found no genetic evidence of these dispersal routes. Our results provide information of particular relevance to these questions.

The Giles Corridor, proposed by Pianka (1972), has been central to these studies investigating dispersal routes through the western sand desert. This corridor of *Acacia* shrublands links the east Murchison goldfields region in Western Australia to the Central Ranges by extending through the Lake Carnegie region in the Great Victoria Desert and the southern part of the Gibson Desert (Van Oosterzee, 1991). Our data, however, find no evidence of a dispersal route via the Giles Corridor during the Pleistocene, with relaxed molecular clock analyses providing support for divergences and secondary contact that pre-date the Pleistocene sand deserts. In addition, we found no evidence of historic hybridization, gene flow or introgression between *C. c. graafi* and *C. c. mensarum*, as would be expected if the Giles Corridor had been the dispersal route. This result seems logical as *C. caudicinctus* is a rock-specialist for which *Acacia* shrublands would not provide an ideal habitat-type for dispersal. Instead, our results, provide evidence of a more northerly historical dispersal route from the Central Ranges to the far EP, at the western and northern edges of the Little Sandy Desert (Fig. 1), with historic phylogenetic connections between the Central Ranges and the far EP. We also find, using ENM, that there are currently suitable climatic conditions and habitat distributions between the Central Ranges and the far EP for potential dispersal routes for the rock-specialists.

A number of rock-dwelling gecko species have been found to have sister lineages in the Central Ranges and the Pilbara (e.g. Oliver et al., 2010; Pepper et al., 2011a,b). In fact, in the saxicolous gecko *Heteronotia spelea* the sister lineages in the Central Ranges and Pilbara (now *H. fasciolatus* – Pepper et al., 2013) were found to have diverged in the Pliocene or early Pleistocene (Pepper et al., 2011a). The age of this divergence is similar to the estimates we provide for the age of the common mtDNA ancestor of *C. c. graafi* in the Central Ranges and the *C. c. caudicinctus* populations from the far EP (Table 3). The formation of the Australian sand deserts are younger than these Pliocene divergences, with luminescence dating estimating dune activity in Australia to at least 300 ka and cosmogenic isotope dating revealing that dune-fields in the western part of the Simpson Deserts began to form 1 Ma (Fujioka & Chappell, 2010). Consequently, the phylogeographical patterns observed in both the dragon lizards and geckos pre-dates the formation of sand deserts. Results from our study suggest that the major lineages (eastern and western) of the *C. caudicinctus* species complex
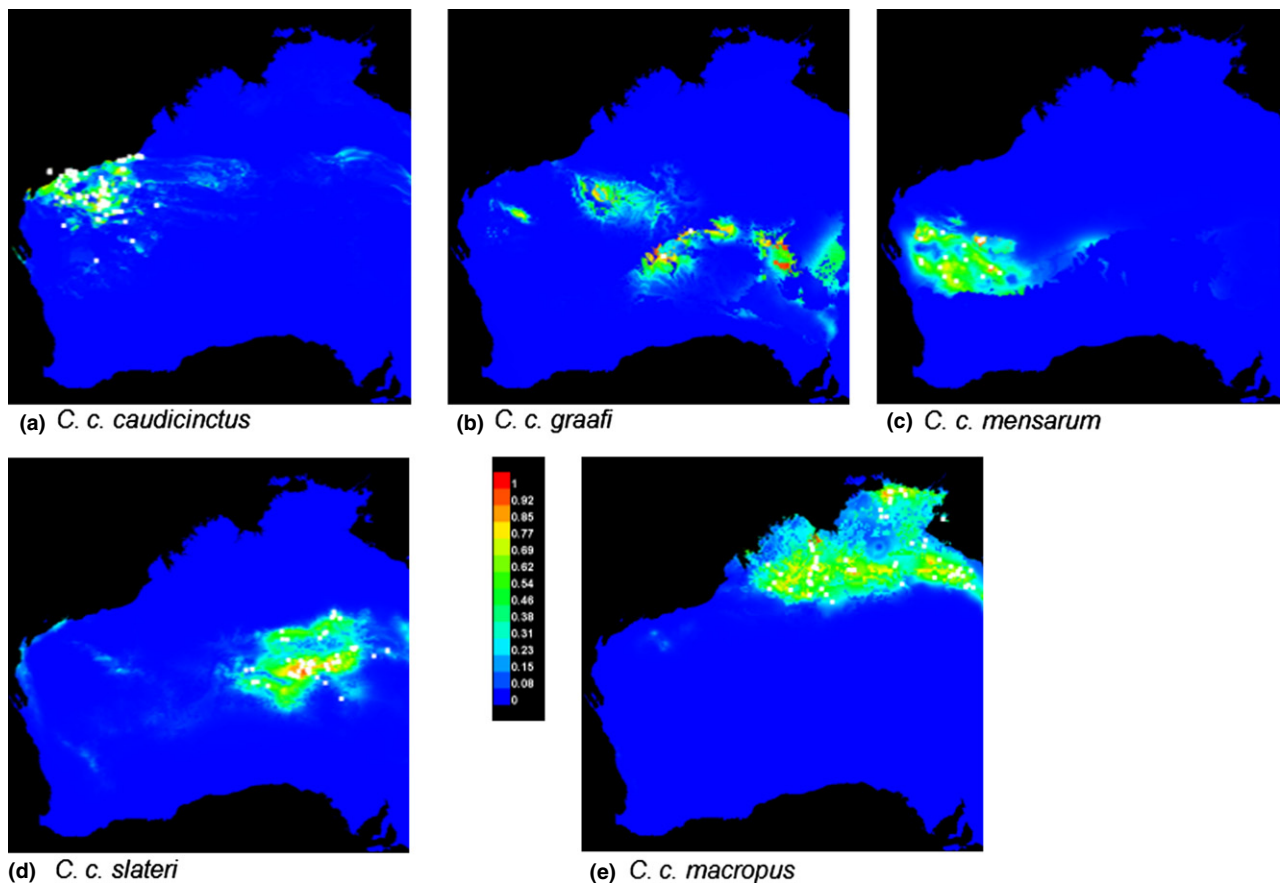
Figure 3 Predicted distributions of *Ctenophorus* subspecies as modelled by MAXENT (Phillips *et al.*, 2006). Warmer colours represent greater predicted environmental suitability with dark blue representing regions not suitable for the species. White dots are locality records.

diverged in the late Miocene, with later secondary contact during the Pliocene, through the Gibson Desert and Little Sandy Desert region.

The Miocene was a time of dramatic climatic shifts, with increasing aridity and seasonality (Byrne *et al.*, 2008) and the Western Australian lowland basins experienced an end to the warmer and wetter conditions of the early Miocene (Martin, 2006). Although a continuous geological record for the period is not available, the late Miocene would have continued to change with increasing aridity through the region (Hill, 1994; Byrne *et al.*, 2008). It is probable that in the late Miocene conditions were unfavourable in the lowlands for species that had occurred there earlier, fragmenting populations as they took refuge in the rocky uplands of the Pilbara and central Australia (Pepper *et al.*, 2011a). In the Pliocene there was a 'mesic pulse', with a temporary return to wet and warm conditions (Byrne *et al.*, 2008). Thus, it is possible that these climatic changes were the major drivers of the phylogeographical patterns observed in the *C. caudicinctus* species complex rather than the expansion of the sand deserts. Increasing Miocene aridity may underlie the original divergence of *C. caudicinctus* into an eastern and western lineage, with a temporary return to mesic conditions in the Pliocene

allowing dispersal and secondary contact with gene exchange between the Central Ranges and Pilbara.

The spread of the sand deserts during the Pleistocene has probably limited subsequent dispersal and gene exchange within the *C. caudicinctus* species complex. However, our ENM, which included a sand layer, does suggest that there are potentially suitable habitats for *C. c. graafi* across the Little Sandy Desert and Gibson Desert into the EP. In fact, the distribution of suitable habitats based on ENM is in concordance with our genetic results. The genetic markers we used in our study provide a snapshot of historic gene exchange, while the ENM suggest that there may be suitable habitats through the western deserts currently. Thus, it would be of particular interest to use genetic markers to explore whether there is infrequent dispersal and gene exchange occurring currently. Further sampling in the rocky habitats through the Gibson Desert area would provide additional important data, if *C. c. caudicinctus* or *C. c. graafi* occur in these areas.

Phylogenetic relationships

Our molecular work, incorporating both mitochondrial and nuclear gene regions, reveal a complex evolutionary and bio-
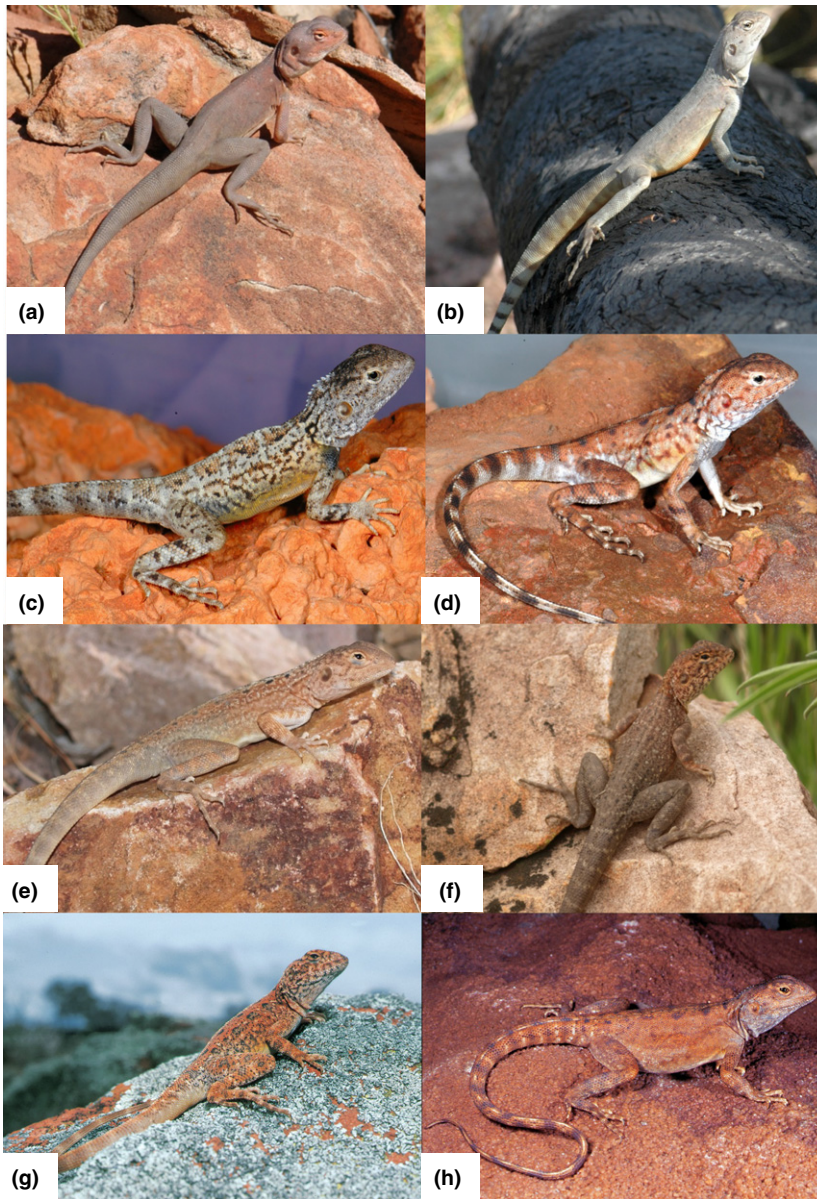
Figure 4 Photographs of each of the *Ctenophorus caudicinctus* subspecies, including two images each of *C. c. caudicinctus* and *C. c. macropus* to demonstrate variation within lineages. Locality information: (a) *C. c. macropus*, Wolfe Creek Crater, Western Australia (image: R. Glor); (b) *C. c. macropus*, western Arnhem Land, Northern Territory (image: R. Glor); (c) *C. c. caudicinctus*, 80 mile beach, Western Australia (image: J. Melville); (d) *C. c. caudicinctus*, Port Headland, Western Australia (image: J. Melville); (e) *C. c. graafi*, Pungkulpirri, Western Australia (image: M. Hutchinson); (f) *C. c. slateri*, Waterhouse Range, Northern Territory (image: M. Hutchinson); (g) *C. c. infans*, Laverton, Western Australia (image: G. Harold); (h) *C. c. mensarum*, Meekatharra, Western Australia (image: G. Gaikhorst).

geographical history in *Ctenophorus caudicinctus*. Using a Bayesian framework for subspecies tree estimation, which is the most appropriate approach when there is conflict between gene trees (see Heled & Drummond, 2010), we provide evidence of phylogenetic congruence between data sets and the unexpectedly deep genetic divergences between subspecies, which suggests that a revision of *C. caudicinctus* subspecies is warranted.

Our genetic data support a close relationship between *C. c. caudicinctus* and *C. c. mensarum*, with no evidence that these subspecies are independent evolutionary lineages. However, we provide strong support that these two subspecies together form an independent evolutionary lineage (with the exception of the two far eastern populations of *C. c. caudicinctus*, which we address further down), which diverged from *C. c. infans* in the late Miocene. *Ctenophorus c. infans* is morphologically distinct, comprising the smallest of the sub-

species with adult male coloration differing little from females and juveniles (Storr, 1967; Fig. 4). Thus, based on both morphological and molecular evidence, we recommend that *C. c. infans* and *C. c. caudicinctus* be raised to full species level and that *C. c. mensarum* should be synonymized into *C. caudicinctus*.

The monophyly of the eastern lineages of *C. caudicinctus* are strongly supported in the mtDNA and species tree analyses, with the inclusion of the far EP populations (discussed below). Morphologically, there is significant variation between *C. c. macropus* and *C. c. slateri* (Storr, 1967; Fig. 4); however, there is also within-lineage diversity, both in terms of genetic diversity (Fig. 1) and morphological variation (Storr, 1967; Fig. 4). There is clearly a need for further research into the diversity within and between these two lineages. For the moment, we recommend raising this lineage as a whole (*C. c. macropus*

and *C. c. slateri*) to species level, with precedence requiring it to become *C. slateri* (Storr, 1967), while *C. c. macropus* is synonymized into *C. slateri*, but with the obvious need of reviewing the diversity within this group in the immediate future.

Finally, we found evidence of historic gene exchange between the eastern and western lineages of *C. caudicinctus*. In particular, two populations in the far EP region, identified as *C. c. caudicinctus,* were supported as belonging to the eastern clade across two gene regions (*ND2* and *BACH1*; Fig. 2). Our results are unable to shed light on whether *C. c. graafi* is the result of gene exchange between *C. c. slateri* and *C. c. caudicinctus* (i.e. a hybrid origin) or whether *C. c. graafi* diverged independently with subsequent gene exchange with *C. c. caudicinctus*. Storr (1967) describes *C. c. graafi* as having morphological characters that differ from either *C. c. caudicinctus* or *C. c. slateri*, thus, further work incorporating more loci (e.g. next generation sequencing) should shed light on the origins of *C. c. graafi*. Until then we recommend the *C. c. graafi* be raised to species level, reflecting its morphological difference, isolated distribution and genetic distinctiveness.

With our recommendations the *C. caudicinctus* species group, which currently incorporates six subspecies, would become four species: *C. caudicinctus, C. infans, C. slateri* and *C. graafi*. However, we acknowledge that further work is required, particularly for *C. slateri* and *C. graafi*.

CONCLUSIONS

The *Ctenophorus caudicinctus* species complex represents an important test case for investigations of phylogeographical structure of species spanning western sand deserts, as it provides the first genetic evidence of biogeographical dispersal routes, which are also supported by ENM. We were able to show that there has been a historic dispersal route between the Central Ranges and Pilbara, probably during the Pliocene, but we found no evidence that the previously hypothesized Giles Corridor has been used as a dispersal route for *C. caudicinctus*. Our results further highlight the biogeographical connection between the Central Ranges and Pilbara and provide additional evidence that divergences in specialist rock-dwelling lizards in this region pre-date the Pleistocene sand deserts.

ACKNOWLEDGEMENTS

REFERENCES

Byrne, M., Yeates, D.K., Joseph, L., Kearney, M., Bowler, J., Williams, M.A.J., Cooper, S., Donnellan, S.C., Keogh, J.S., Leys, R., Melville, J., Murphy, D.J., Porch, N. & Wyrwoll, K.-H. (2008) Birth of a biome: insights into the assembly and maintenance of the Australian arid zone biota. *Molecular Ecology*, **17**, 4398–4417.

Chapple, D.G., Keogh, J.S. & Hutchinson, M.N. (2004) Molecular phylogeography and systematics of the arid-zone members of the *Egernia whitii* (Lacertilia: Scincidae) species group. *Molecular Phylogenetics and Evolution*, **33**, 549–561.

Covacevich, J., Couper, P., Molnar, R.E., Witten, G. & Young, W. (1990) Miocene dragons from Riversleigh: new data on the history of the family Agamidae (Reptilia: Squamata) in Australia. *Memoirs of the Queensland Museum*, **29**, 339–360.

Drummond, A.J., Ho, S.Y.W., Phillips, M.J. & Rambaut, A. (2006) Relaxed phylogenetics and dating with confidence. *PLoS Biology*, **4**, e88.

Edwards, D.L. & Melville, J. (2011) Extensive phylogeographic and morphological diversity in *Diporiphora nobbi* (Agamidae) leads to a taxonomic review and a new species description. *Journal of Herpetology*, **45**, 530–546.

Elith, J., Phillips, S.J., Hastie, T., Dudík, M., Chee, Y.E. & Yates, C.J. (2011) A statistical explanation of MaxEnt for ecologists. *Diversity and Distributions*, **17**, 43–57.

Felsenstein, J. (1985) Confidence limits on phylogenies: an approach using the bootstrap. *Evolution*, **39**, 783–791.

Fordham, D.A., Akçakaya, H.R., Araújo, M.B. & Brook, B.W. (2012) Modelling range shifts for invasive vertebrates in response to climate change. *Wildlife conservation in a changing climate* (ed. by J.F. Brodie, E.S. Post and D.F. Doak), pp. 86–108. University of Chicago Press, Chicago, IL.

Fujioka, T. & Chappell, J. (2010) History of Australian aridity: chronology in the evolution of arid landscapes. *Australian landscapes* (ed. by P. Bishop and B. Pillans). *Geological Society, London, Special Publications*, **346**, 121–139.

Guindon, S. & Gascuel, O. (2003) A simple, fast, and accurate algorithm to estimate large phylogenies by maximum likelihood. *Systematic Biology*, **52**, 696–704.

Heled, J. & Drummond, A.J. (2010) Bayesian inference of species trees from multilocus data. *Molecular Biology and Evolution*, **27**, 570–580.

Hill, R.S. (1994) *The history of Australian vegetation and flora: Cretaceous to recent*. Cambridge University Press, Cambridge.

Kozak, K.H., Graham, C.H. & Wiens, J.J. (2008) Integrating GIS-based environmental data into evolutionary biology. *Trends in Ecology and Evolution*, **23**, 141–148.

Macey, J.R., Larson, A., Ananjeva, N.B. & Pupenfuss, T.J. (1997) Replication slippage may cause parallel evolution in the secondary structures of mitochondrial transfer RNAs. *Molecular Biology and Evolution*, **14**, 30–39.

Martin, H.A. (2006) Cenozoic climatic changes and the development of the arid vegetation of Australia. *Journal of Arid Environments*, **66**, 533–563.

McMahon, J.P., Hutchinson, M.F., Nix, H.A. & Ord, K.D. (1995) *ANUCLIM User's Guide, Version 1.* Centre for Resource and Environmental Studies, Australian National University, Canberra.

Melville, J. & Hale, J.M. (2009) Length variation in the N-terminal domain of the recombination-activating gene 1 (Rag1) across squamates. *Molecular Phylogenetics and Evolution*, **52**, 898–903.

Melville, J., Schulte, J.A., II & Larson, A. (2001) A molecular phylogenetic study of ecological diversification in the Australian lizard genus Ctenophorus. *Journal of Experimental Zoology (Molecular Development and Evolution)*, **291**, 339–353.

Melville, J., Ritchie, E.G., Chapple, S.N.J., Glor, R.E. & Schulte, J.A. (2011) Evolutionary origins and diversification of dragon lizards in Australia's tropical savannas. *Molecular Phylogenetics and Evolution*, **58**, 257–270.

Milá, B., Surget-Groba, Y., Heulin, B., Gosá, A. & Fitze, P.S. (2013) Multilocus phylogeography of the common lizard Zootoca vivipara at the Ibero-Pyrenean suture zone reveals lowland barriers and high-elevation introgression. *BMC Evolutionary Biology*, **13**, 1–15.

Oliver, P.M., Adams, M. & Doughty, P. (2010) Molecular evidence for ten species and Oligo-Miocene vicariance within a nominal Australian gecko species (Crenadactylus ocellatus, Diplodactylidae). *BMC Evolutionary Biology*, **10**, 386.

Pepper, M., Fujita, M.K., Moritz, C. & Keogh, J.S. (2011a) Palaeoclimate change drove diversification among isolated mountain refugia in the Australian arid zone. *Molecular Ecology*, **20**, 1529–1545.

Pepper, M., Ho, S.Y.W., Fujita, M.K. & Keogh, J.S. (2011b) The genetic legacy of aridification: climate cycling fostered lizard diversification in Australian montane refugia and left low-lying deserts genetically depauperate. *Molecular Phylogenetics and Evolution*, **61**, 750–759.

Pepper, M., Doughty, P., Fujita, M.K., Moritz, C. & Keogh, J.S. (2013) Speciation on the rocks: integrated systematics of the Heteronotia spelea species complex (Gekkota; Reptilia) from Western and Central Australia. *PLoS ONE*, **8**, e78110. doi:10.1371/journal.pone.0078110.

Phillips, S.J., Anderson, R.P. & Schapire, R.E. (2006) Maximum entropy modeling of species geographic distributions. *Ecological Modelling*, **190**, 231–259.

Pianka, E.R. (1972) Zoogeography and speciation of Australian Desert Lizards: and ecological perspective. *Copeia*, **1972**, 127–145.

Rambaut, A. & Drummond, A. (2003). *Tracer: MCMC trace analysis tool.* University of Oxford, Oxford, UK.

Ritchie, E.G., Martin, J.K., Krockenberger, A.K., Garnett, S. & Johnson, C.N. (2008) Large-herbivore distribution and abundance: intra-and interspecific niche variation in the tropics. *Ecological Monographs*, **78**, 105–122.

Ronquist, F., Teslenko, M., van der Mark, P., Ayres, D.L., Darling, A., Höhna, S., Larget, B., Liu, L., Suchard, M.A. & Huelsenbeck, J.P. (2012) MrBayes 3.2: efficient Bayesian phylogenetic inference and model choice across a large model space. *Systematic Biology*, **61**, 539–542.

Schulte, J.A., II, Melville, J. & Larson, A. (2003) Molecular phylogenetic evidence for ancient divergence of lizard taxa either side of Wallace's Line. *Proceedings of the Royal Society B: Biological Sciences*, **270**, 597–603.

Shoo, L.P., Rose, R., Doughty, P., Austin, J.J. & Melville, J. (2008) Diversification patterns of pebble-mimic dragons are consistent with historical disruption of important habitat corridors in arid Australia. *Molecular Phylogenetics and Evolution*, **48**, 528–542.

Storr, G.M. (1967) Geographic races of the agamid lizard Amphibolurus caudicinctus. *Journal of the Royal Society of Western Australia*, **50**, 49–56.

Storr, G.M., Johnstone, R.E. & Smith, L.A. (1983) *Lizards of Western Australia. II, Dragons and monitors.* Western Australian Museum, Perth, WA.

Van Oosterzee, P. (1991) *The Centre: the natural history of Australia's desert regions.* William Heinemann/Reed Books, Sydney, Australia.

SUPPORTING INFORMATION

Additional Supporting Information may be found in the online version of this article:

Appendix S1 Details of *Ctenophorus caudicinctus* and *C. ornatus* samples.

Appendix S2 Supplementary materials and methods, including primers and PCR protocols.

Appendix S3 Supplementary figures, including Bayesian trees for each of the five nuclear genes.

BIOSKETCH

Jane Melville studies the evolution, systematics and eco-morphology of Australian agamids. Her research focuses on understanding adaptive responses of agamids to environmental change and the evolutionary mechanisms underlying these changes.

Author contributions: J.M. and J.H. initiated the research; J.M. and E.R. conceived the ideas; J.M., M.H. J.H. and S.C. acquired the data; J.M. and E.R. analysed the data; J.M. led the writing; M.H. J.H., S.C. and E.R. contributed to the writing; all authors discussed the ideas and commented on the manuscript.

Editor: Fumin Lei

Concordance in phylogeography and ecological niche modelling identify dispersal corridors for reptiles in arid Australia.

Jane Melville, Margaret L. Haines, Joshua Hale, Stephanie N. J. Chapple, and Euan G. Ritchie

Appendix S1 Supplementary table

Table S1. Details of *Ctenophorus caudicinctus* and *C. ornatus* samples used in genetic analyses. Museum acronyms are as follows: WAM, Western Australian Museum; NMV, Museum Victoria; SAMA, South Australian Museum; ANWC, Australian National Wildlife Collection.

Museum	ID	Taxon	*ND2*	*BACH1*	*BDNF*	*GAPD*	*NTF3*	*PRLR*
NMVD	74360	*C. c. caudicinctus*	KU187613	-	-	-	-	-
NMVD	74373	*C. c. caudicinctus*	KU187614	-	-	-	-	-
NMVD	74374	*C. c. caudicinctus*	KU187615	KU187421	KU187533	KU187827	KU187796	KU187697
NMVD	74376	*C. c. caudicinctus*	KU187617	-	-	-	-	-
NMVD	74377	*C. c. caudicinctus*	KU187619	-	-	-	-	-
NMVD	74378	*C. c. caudicinctus*	KU187616	-	-	-	-	-
NMVD	74379	*C. c. caudicinctus*	KU187618	-	-	-	-	-
NMVD	74380	*C. c. caudicinctus*	KU187621	KU187448	KU187525	KU187828	KU187760	-
NMVD	74381	*C. c. caudicinctus*	KU187620	-	-	-	-	-
NMVD	74385	*C. c. caudicinctus*	KU187622	KU187463	KU187523	KU187829	KU187759	KU187700
NMVD	74386	*C. c. caudicinctus*	KU187623	-	-	-	-	-
NMVD	74394	*C. c. caudicinctus*	KU187624	KU187435	KU187532	KU187830	KU187773	KU187707
NMVD	74395	*C. c. caudicinctus*	KU187625	-	-	-	-	-
NMVD	74396	*C. c. caudicinctus*	KU187626	KU187458	KU187548	KU187831	KU187776	KU187701
WAMR	100663	*C. c. caudicinctus*	KU187677	-	-	-	-	-
WAMR	100788	*C. c. caudicinctus*	KU187575	-	-	-	-	-
WAMR	102084	*C. c. caudicinctus*	KU187576	KU187438	KU187494	KU187838	KU187815	KU187702
WAMR	102611	*C. c. caudicinctus*	KU187577	KU187470	KU187499	KU187839	KU187763	KU187698
WAMR	102612	*C. c. caudicinctus*	KU187578	-	-	-	-	-
WAMR	102635	*C. c. caudicinctus*	KU187579	KU187455	KU187500	KU187840	KU187764	KU187703
WAMR	104099	*C. c. caudicinctus*	KU187681	-	-	-	-	-
WAMR	104102	*C. c. caudicinctus*	KU187580	KU187460	KU187481	KU187841	KU187758	KU187740
WAMR	108607	*C. c. caudicinctus*	KU187582	-	-	-	-	-
WAMR	108610	*C. c. caudicinctus*	KU187583	-	-	-	-	-
WAMR	110815	*C. c. caudicinctus*	KU187586	-	-	-	-	-
WAMR	110831	*C. c. caudicinctus*	KU187587	KU187462	KU187530	KU187847	KU187791	KU187704
WAMR	114346	*C. c. caudicinctus*	KU187589	-	-	-	-	-
WAMR	114349	*C. c. caudicinctus*	KU187590	-	-	-	-	-
WAMR	114351	*C. c. caudicinctus*	KU187591	KU187454	KU187531	KU187849	KU187765	KU187705
WAMR	114353	*C. c. caudicinctus*	KU187592	-	-	-	-	-
WAMR	114355	*C. c. caudicinctus*	KU187593	-	-	-	-	-
WAMR	114547	*C. c. caudicinctus*	KU187594	KU187469	KU187524	KU187850	KU187793	KU187741
WAMR	119937	*C. c. caudicinctus*	KU187599	-	-	-	-	-
WAMR	125738	*C. c. caudicinctus*	KU187602	-	-	-	-	-
WAMR	127832	*C. c. caudicinctus*	KU187604	-	-	-	-	-
WAMR	131013	*C. c. caudicinctus*	KU187605	KU187416	KU187543	-	KU187810	KU187746
WAMR	139008	*C. c. caudicinctus*	KU187630	-	-	-	-	-
WAMR	139022	*C. c. caudicinctus*	KU187631	-	-	-	-	-
WAMR	139051	*C. c. caudicinctus*	KU187632	KU187476	KU187541	KU187869	KU187787	
WAMR	139261	*C. c. caudicinctus*	KU187633	KU187477	KU187540	KU187870	KU187792	KU187735
WAMR	140317	*C. c. caudicinctus*	KU187634	-	-	-	-	-
WAMR	140345	*C. c. caudicinctus*	KU187635	-	-	-	-	-
WAMR	141337	*C. c. caudicinctus*	KU187636	KU187479	KU187547	KU187871	KU187814	KU187736
WAMR	154125	*C. c. caudicinctus*	KU187637	-	-	-	-	-
WAMR	154126	*C. c. caudicinctus*	KU187638	-	-	-	-	-
WAMR	154127	*C. c. caudicinctus*	KU187639	-	-	-	-	-
WAMR	154128	*C. c. caudicinctus*	KU187640	-	-	-	-	-
WAMR	154129	*C. c. caudicinctus*	KU187641	KU187419	KU187538	KU187873	KU187804	KU187706
WAMR	154312	*C. c. caudicinctus*	KU187674	KU187427	KU187537	KU187874	KU187805	KU187737

WAMR	154313	*C. c. caudicinctus*	KU187642	-	-	-	-	-
WAMR	154516	*C. c. caudicinctus*	KU187643	KU187426	KU187536	KU187876	KU187806	KU187731
WAMR	154519	*C. c. caudicinctus*	KU187676	-	-	-	-	-
WAMR	154520	*C. c. caudicinctus*	KU187644	-	-	-	-	-
WAMR	154521	*C. c. caudicinctus*	KU187645	KU187418	KU187534	KU187875	KU187807	KU187699
WAMR	156595	*C. c. caudicinctus*	KU187646	KU187425	KU187535	KU187878	KU187809	KU187732
WAMR	144332	*C. c. graafi*	KU187675	KU187480	KU187539	KU187872	KU187803	KU187738
SAMAR	91440	*C. c. graafi*	KU187570	KU187459	KU187529	-	KU187775	KU187708
SAMAR	91551	*C. c. graafi*	KU187573	KU187445	KU187526	KU187881	KU187785	KU187710
SAMAR	91478	*C. c. graafi*	KU187571	KU187428	KU187527	KU187880	KU187801	KU187744
SAMAR	91543	*C. c. graafi*	KU187572	-	-	-	-	-
SAMAR	91573	*C. c. graafi*	KU187574	-	-	-	-	-
SAMAR	91400	*C. c. graafi*	KU187679	-	-	-	-	-
SAMAR	91441	*C. c. graafi*	KU187671	KU187429	KU187528	KU187879	KU187800	KU187709
WAMR	119039	*C. c. infans*	KU187596	KU187444	KU187495	KU187854	KU187784	KU187696
WAMR	119040	*C. c. infans*	KU187597	-	-	-	-	-
WAMR	119041	*C. c. infans*	KU187598	KU187437	KU187497	KU187855	KU187769	KU187695
ANWCR	146831	*C. c. infans*	KU187569	KU187413	KU187496	KU187818	KU187752	KU187694
NMVD	72577	*C. c. macropus*	KU187550	KU187424	KU187503	KU187819	KU187802	KU187711
NMVD	72581	*C. c. macropus*	KU187549	-	-	-	-	-
NMVD	72611	*C. c. macropus*	KU187551	-	-	-	-	-
NMVD	72613	*C. c. macropus*	KU187552	-	-	-	-	-
NMVD	72614	*C. c. macropus*	KU187553	-	-	-	-	-
NMVD	72670	*C. c. macropus*	KU187557	-	-	-	-	-
NMVD	72679	*C. c. macropus*	KU187559	-	-	-	-	-
NMVD	72687	*C. c. macropus*	KU187556	-	-	-	-	-
NMVD	72688	*C. c. macropus*	KU187558	KU187414	KU187515	KU187820	KU187756	KU187727
NMVD	73882	*C. c. macropus*	KU187560	KU187441	KU187514	KU187821	KU187799	KU187712
NMVD	73937	*C. c. macropus*	KU187561	KU187450	KU187513	KU187822	KU187762	KU187713
NMVD	73949	*C. c. macropus*	KU187562	KU187440	KU187512	-	KU187780	KU187714
NMVD	73961	*C. c. macropus*	KU187563	KU187452	KU187511	KU187823	KU187772	KU187715
WAMR	108736	*C. c. macropus*	KU187584	-	-	-	-	-
WAMR	108814	*C. c. macropus*	KU187585	-	-	-	-	-
WAMR	113989	*C. c. macropus*	KU187588	KU187439	KU187509	KU187848	KU187768	KU187730
WAMR	125199	*C. c. macropus*	KU187600	KU187472	KU187504	KU187857	KU187789	KU187717
WAMR	125200	*C. c. macropus*	KU187601	KU187473	KU187507	KU187858	KU187783	KU187718
WAMR	132853	*C. c. macropus*	KU187608	KU187447	KU187508	KU187862	KU187770	KU187719
WAMR	132854	*C. c. macropus*	KU187609	KU187415	KU187510	KU187863	KU187811	KU187720
WAMR	132855	*C. c. macropus*	KU187610	-	-	-	-	-
NMVD	74055	*C. c. macropus*	KU187564	KU187430	KU187505	KU187824	KU187751	KU187739
NMVD	74056	*C. c. macropus*	KU187565	-	-	-	-	-
NMVD	74057	*C. c. macropus*	KU187566	-	-	-	-	-
NMVZ	18935	*C. c. macropus*	KU187554	KU187442	KU187502	KU187833	KU187749	KU187716
NMVZ	18937	*C. c. macropus*	KU187555	KU187422	KU187501	KU187834	KU187750	KU187721
NMVD	74398	*C. c. mensarum*	KU187627	KU187464	KU187522	KU187832	KU187797	KU187743
WAMR	106139	*C. c. mensarum*	KU187581	KU187449	KU187519	KU187846	KU187755	KU187722
WAMR	116891	*C. c. mensarum*	KU187682	KU187468	KU187498	KU187851	KU187795	KU187745
WAMR	116892	*C. c. mensarum*	KU187678	-	-	-	-	-
WAMR	117034	*C. c. mensarum*	KU187595	-	-	-	-	-
WAMR	123851	*C. c. mensarum*	KU187672	KU187467	KU187520	KU187856	KU187782	KU187723
WAMR	126476	*C. c. mensarum*	KU187603	KU187474	KU187545	KU187859	KU187754	KU187724
WAMR	127024	*C. c. mensarum*	KU187673	-	-	-	-	-
WAMR	131781	*C. c. mensarum*	KU187606	-	-	-	-	-
WAMR	131782	*C. c. mensarum*	KU187607	KU187475	KU187518	KU187861	KU187777	KU187742
WAMR	136265	*C. c. mensarum*	KU187628	-	-	-	-	-
WAMR	136272	*C. c. mensarum*	KU187629	-	-	-	-	-
WAMR	136285	*C. c. mensarum*	KU187680	KU187478	KU187521	KU187868	KU187816	KU187748
NMVD	74268	*C. c. slateri*	KU187611	KU187466	KU187506	KU187825	KU187771	KU187728
NMVD	74284	*C. c. slateri*	KU187612	KU187433	KU187516	KU187826	KU187774	KU187726
ANWCR	6140	*C. c. slateri*	KU187567	-	-	-	-	-

ANWCR	6144	*C. c. slateri*	KU187568	KU187431	KU187517	KU187817	KU187753	KU187725
WAMR	77978	*C. ornatus*	KU187647	KU187465	KU187482	KU187835	KU187788	KU187685
WAMR	77979	*C. ornatus*	KU187648	-	-	-	-	-
WAMR	84713	*C. ornatus*	KU187649	KU187457	KU187483	KU187836	KU187786	KU187686
WAMR	84714	*C. ornatus*	KU187650	-	-	-	-	-
WAMR	96602	*C. ornatus*	KU187651	KU187451	KU187489	KU187837	KU187781	KU187684
WAMR	103881	*C. ornatus*	KU187652	KU187434	KU187484	KU187842	KU187790	KU187687
WAMR	103884	*C. ornatus*	KU187653	KU187461	KU187546	KU187843	KU187761	KU187733
WAMR	103885	*C. ornatus*	KU187654	-	-	-	-	-
WAMR	103886	*C. ornatus*	KU187655	KU187443	KU187486	KU187844	KU187798	KU187729
WAMR	104404	*C. ornatus*	KU187656	KU187471	KU187490	KU187845	KU187757	KU187688
WAMR	117278	*C. ornatus*	KU187657	-	-	-	-	-
WAMR	117279	*C. ornatus*	KU187658	KU187446	KU187487	KU187852	KU187766	KU187692
WAMR	117360	*C. ornatus*	KU187659	KU187453	KU187485	KU187853	KU187794	KU187689
WAMR	127596	*C. ornatus*	KU187660	-	-	-	-	-
WAMR	127599	*C. ornatus*	KU187661	-	-	-	-	-
WAMR	127600	*C. ornatus*	KU187662	-	-	-	-	-
WAMR	127601	*C. ornatus*	KU187663	KU187456	KU187544	KU187860	KU187767	KU187690
WAMR	132907	*C. ornatus*	KU187664	KU187432	KU187493	KU187865	KU187778	KU187747
WAMR	132911	*C. ornatus*	KU187665	-	-	-	-	-
WAMR	132912	*C. ornatus*	KU187666	KU187417	KU187492	KU187864	KU187812	KU187693
WAMR	135661	*C. ornatus*	KU187667	KU187436	KU187491	KU187866	KU187779	KU187734
WAMR	135662	*C. ornatus*	KU187668	KU187423	KU187542	KU187867	KU187813	KU187683
WAMR	154798	*C. ornatus*	KU187669	KU187420	KU187488	KU187877	KU187808	KU187691
WAMR	157794	*C. ornatus*	KU187670	-	-	-	-	-

Concordance in phylogeography and ecological niche modelling identify dispersal corridors for reptiles in arid Australia.

Jane Melville, Margaret L. Haines, Joshua Hale, Stephanie Chapple, and Euan G. Ritchie

Appendix S2 Supplementary Materials and Methods

Table S2. Primers and PCR protocols for all gene regions used in this study.

Locus	Primer sequences (5' - 3')	PCR Protocol	Reference
ND2	tRNA^{Met} 5' AAGCAGTTGGGCCCATRCC 3' COIr.aga 5' AGRGTTCCRATRTCTTTRTGRTT 3'	95°C 15 min; 40x(94°C 20s, 55°C 20s,72°C 90s); 72°C 5 min	F: Macey et al. (2000) R: Modified Macey et al. (1997)
BACH1	CtenBACHf 5' TGCAAGTGTGCTGAGTTTTTG 3' CtenBACHr 5' CTGGGGATCTGGAACACAGT 3'	94°C 2 min; 40x(94°C 30s, 55°C 30s,72°C 45s); 72°C 5 min	Edwards et al. (2015)
BDNF	BDNF-F 5' GACCATCCTTTTCCTKACTATGGTTATTTC 3' BDNF-R 5' CTATCTTCCCCTTTTAATGGTCAGTGTACA 3'	95°C 15 min; 40x(94°C 20s, 48°C 20s,72°C 90s); 72°C 5 min	Modified Leaché and McGuire (2006)
GAPD	GapdL890 5' ACCTTTAATGCGGGTGCTGGCATTGC 3' GapdH950 5' CATCAAGTCCACAACACGGTTGCTGTA 3'	94°C 2 min; 10x[94°C 30s, 60°C 30s (-2°C/2 cycles), 72°C 45s]; 30x(94°C 45s, 48°C 30s, 72°C 45s); 72°C 5 min	Dolman and Phillips (2004)
NTF3	NTF3_f1 5' ATGTCCATCTTGTTTTATGTGATATTT 3' NTF3_r1 5' ACRAGTTTRTTGTTYTCTGAAGTC 3'	94°C 2 min; 40x(94°C 30s, 50°C 30s,72°C 45s); 72°C 5 min	Townsend et al. (2008)
PRLR	Cmac_PRLRf 5' GCCAAGTTGTCAAAAGTGTCA 3' Cmac_PRLRr 5' GCTTTGTGGAHAAGGGAAGG 3'	94°C 2 min; 10x[94°C 30s, 60°C 30s (-2°C/2 cycles), 72°C 45s]; 30x(94°C 45s, 48°C 30s, 72°C 45s); 72°C 5 min	Edwards et al. (2015)

References

Dolman, G., Phillips, B. (2004) Single copy nuclear DNA markers characterized for comparative phylogeography in Australian wet tropics rainforest skinks. *Molecular Ecology Notes*, **4**, 185-187.

Edwards, D. L., Melville, J., Joseph, L., Keogh, J. S. (2015) Ecological divergence, adaptive diversification and the evolution of social signaling traits: an empirical study in arid Australian lizards. *American Naturalist*, in press

Leaché, A. D., McGuire, J. A. (2006) Phylogenetic relationships of horned lizards (*Phrynosoma*) based on nuclear and mitochondrial data: Evidence for a misleading mitochondrial gene tree. *Molecular Phylogenetics and Evolution*, **39**, 628-644.

Macey, J. R., Larson, A., Ananjeva, N. B., Pupenfuss, T. J. (1997) Replication slippage may cause parallel evolution in the secondary structures of mitochondrial transfer RNAs. *Molecular Biology and Evolution*, **14**, 30–39.

Macey, J. R., Schulte, J. A., Larson, A. (2000). Evolution and phylogenetic information content of mitochondrial genomic structural features illustrated with acrodont lizards. *Systematic Biology*, **49**, 257-277.

Townsend, T. M., Alegre, R. E., Kelley, S. T., Wiens, J. J., Reeder, T. W. (2008) Rapid development of multiple nuclear loci for phylogenetic analysis using genomic resources: an example from squamate reptiles. *Molecular phylogenetics and evolution*, **47**, 129-142.

Concordance in phylogeography and ecological niche modelling identify dispersal corridors for reptiles in arid Australia.

Jane Melville, Margaret L. Haines, Joshua Hale, Stephanie Chapple, and Euan G. Ritchie

Appendix S3 Supplementary figures

(a) BACH1
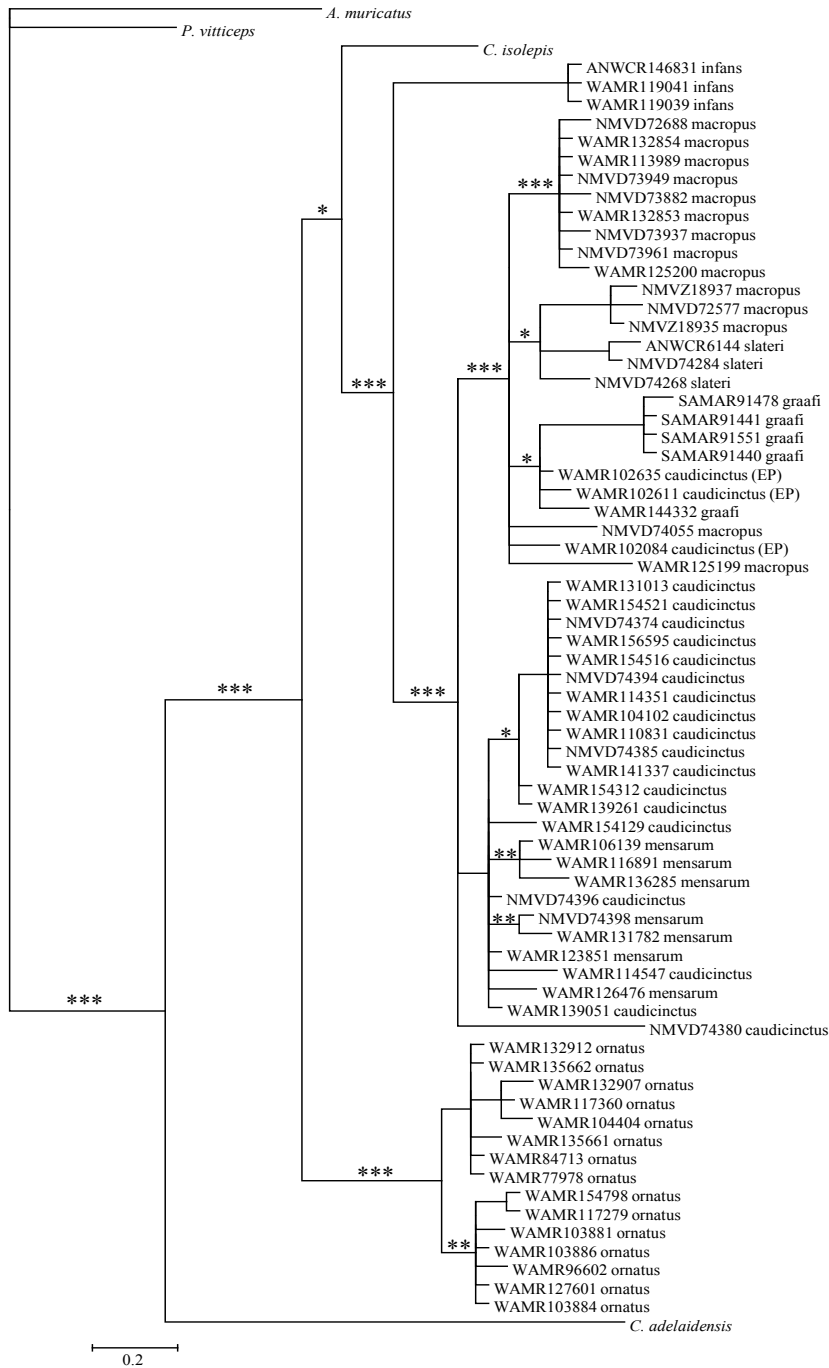
Clade posterior probabilities: *** > 98%; ** 90-97%; * 80-89%.

Figure S1. Bayesian phylogenetic trees from five nuclear genes: (a) *BDNF*; (b) *BACH1*; (c) *GAPD*; (d) *NTF3*; and (e) *PRLR*.

(b) BDNF

Pvitticeps
Amuricatus
Cisolepis
Cadelaidensis
WAMR77978 ornatus
WAMR84713 ornatus
WAMR103881 ornatus
WAMR104404 ornatus
WAMR132912 ornatus
WAMR132907 ornatus
WAMR127601 ornatus
WAMR103884 ornatus
WAMR117360 ornatus
WAMR103886 ornatus
WAMR135661 ornatus
WAMR135662 ornatus
WAMR117279 ornatus
WAMR96602 ornatus
WAMR154798 ornatus
NMVZ18937 macropus
NMVZ18935 macropus
NMVD72577 macropus
WAMR125199 macropus
NMVD74055 macropus
WAMR125200 macropus
WAMR132853 macropus
NMVD73961 macropus
WAMR113989 macropus
WAMR132854 macropus
NMVD73949 macropus
NMVD73937 macropus
NMVD73882 macropus
NMVD72688 macropus
NMVD74268 slateri
NMVD74284 slateri
ANWCR6144 slateri
WAMR102611 caudicinctus (EP)
WAMR102635 caudicinctus (EP)
WAMR102084 caudicinctus (EP)
WAMR144332 graafi
SAMAR91440 graafi
SAMAR91478 graafi
SAMAR91441 graafi
SAMAR91551 graafi
WAMR119039 infans
ANWCR146831 infans
WAMR119041 infans
WAMR116891 mensarum
WAMR126476 mensarum
WAMR123851 mensarum
WAMR136285 mensarum
WAMR106139 mensarum
WAMR114547 caudicinctus
NMVD74380 caudicinctus
WAMR139051 caudicinctus
NMVD74398 mensarum
WAMR131782 mensarum
NMVD74385 caudicinctus
WAMR139261 caudicinctus
WAMR114351 caudicinctus
NMVD74374 caudicinctus
WAMR154516 caudicinctus
WAMR104102 caudicinctus
WAMR110831 caudicinctus
NMVD74394 caudicinctus
WAMR154521 caudicinctus
WAMR154129 caudicinctus
NMVD74396 caudicinctus
WAMR131013 caudicinctus
WAMR156595 caudicinctus
WAMR154312 caudicinctus
WAMR141337 caudicinctus

0.002

Clade posterior probabilities: *** > 98%; ** 90-97%; * 80-89%.

(c) GAPD

A. muricatus

P. vitticeps

C. adelaidensis

C. isolepis

ANWCR6144 slateri
NMVD73937 macropus
NMVD73961 macropus
NMVD74268 slateri
NMVD74398 mensarum
NMVZ18937 macropus
WAMR113989 macropus
WAMR114547 caudicinctus
WAMR116891 mensarum
WAMR123851 mensarum
WAMR125199 macropus
WAMR125200 macropus
WAMR126476 mensarum
WAMR131782 mensarum
WAMR132854 macropus
WAMR136285 mensarum
NMVD73949 macropus
SAMAR91440 graafi
WAMR131013 caudicinctus

** ANWCR146831 infans
WAMR119039 infans
WAMR119041 infans

* WAMR102084 caudicinctus (EP)
WAMR102611 caudicinctus (EP)
WAMR102635 caudicinctus (EP)
WAMR144332 graafi
SAMAR91441 graafi
SAMAR91478 graafi
SAMAR91551 graafi

* NMVD72577 macropus
NMVD74055 macropus
NMVZ18935 macropus

NMVD74284 slateri
WAMR106139 mensarum

NMVD72688 macropus
NMVD73882 macropus
WAMR132853 macropus

NMVD74374 caudicinctus
NMVD74385 caudicinctus
NMVD74394 caudicinctus
NMVD74396 caudicinctus
WAMR104102 caudicinctus
WAMR110831 caudicinctus
WAMR114351 caudicinctus
WAMR139051 caudicinctus
WAMR139261 caudicinctus
WAMR141337 caudicinctus
WAMR154129 caudicinctus
WAMR154312 caudicinctus
WAMR154521 caudicinctus
WAMR154516 caudicinctus
WAMR156595 caudicinctus
NMVD74380 caudicinctus

* WAMR77978 ornatus
WAMR84713 ornatus
WAMR96602 ornatus
** WAMR103881 ornatus
WAMR103886 ornatus
WAMR103884 ornatus
WAMR104404 ornatus
WAMR117279 ornatus
WAMR117360 ornatus
WAMR132912 ornatus
WAMR127601 ornatus
WAMR132907 ornatus
WAMR135661 ornatus
WAMR135662 ornatus
WAMR154798 ornatus

0.001

Clade posterior probabilities: *** > 98%; ** 90-97%; * 80-89%.

(d) NTF3

Clade posterior probabilities: *** > 98%; ** 90-97%; * 80-89%.

(e) PRLR

P. vitticeps
A. muricatus
C. isolepis
WAMR102084 caudicinctus (EP)
WAMR125199 macropus
NMVD74374 caudicinctus
WAMR123851 mensarum
WAMR102611 caudicinctus (EP)
WAMR106139 mensarum
WAMR136285 mensarum
WAMR114547 caudicinctus
WAMR104102 caudicinctus
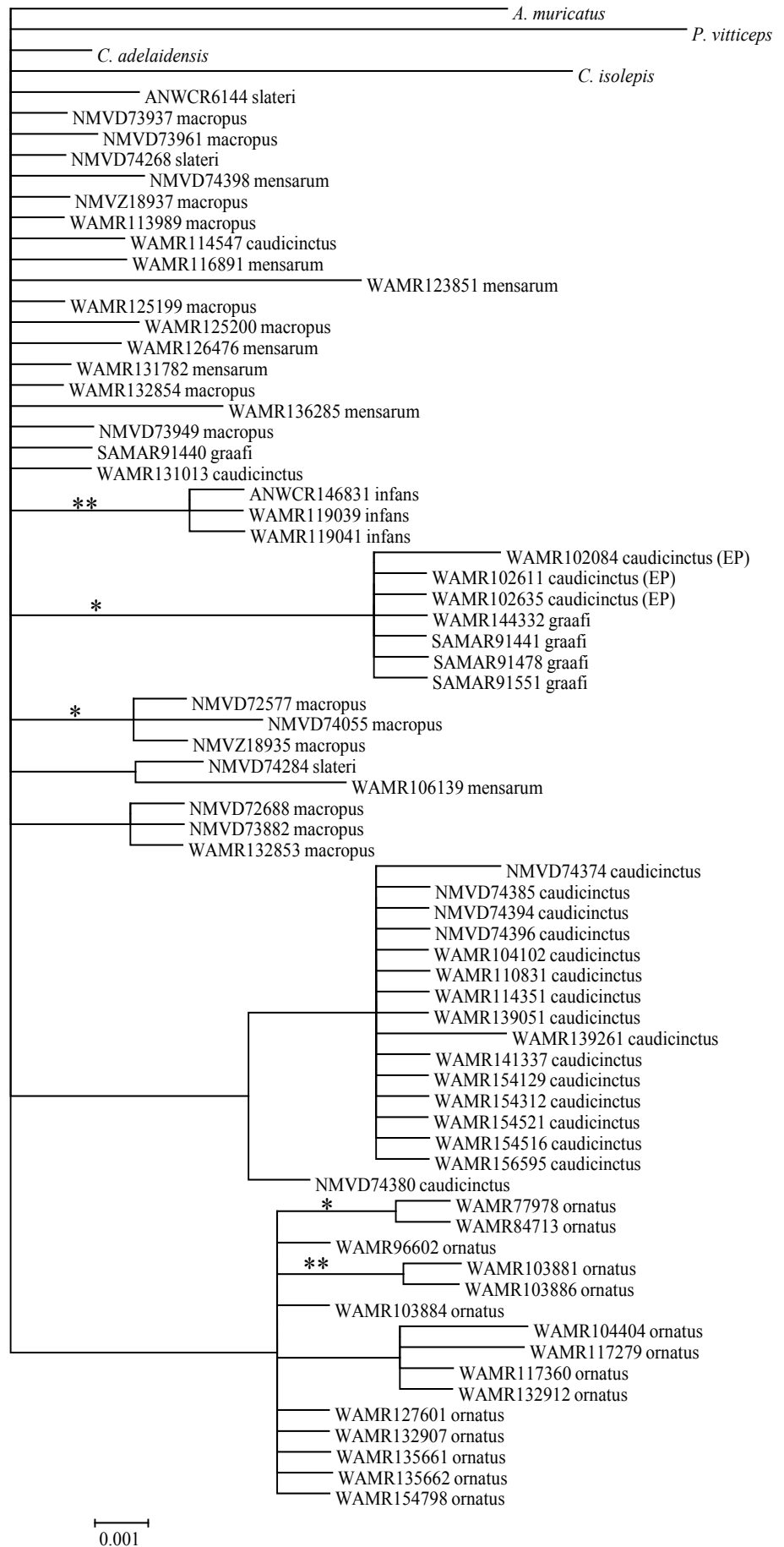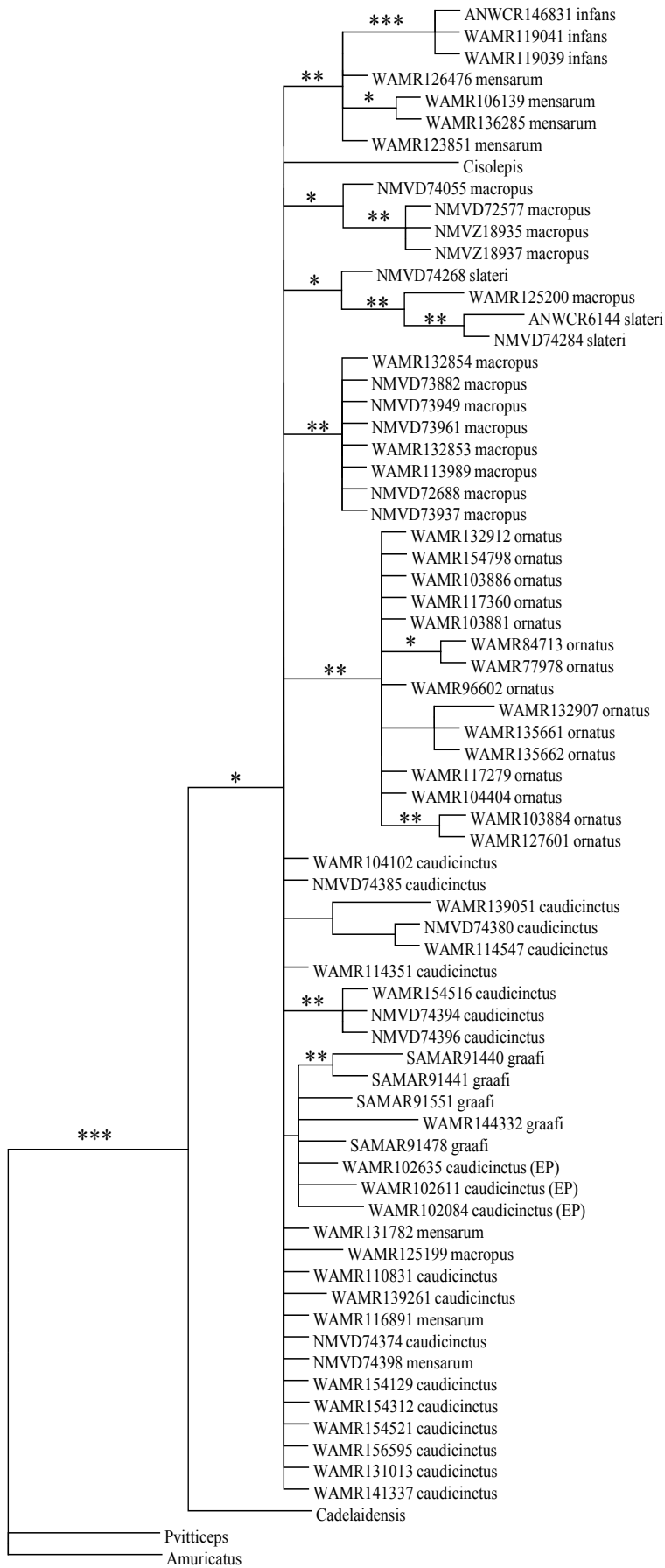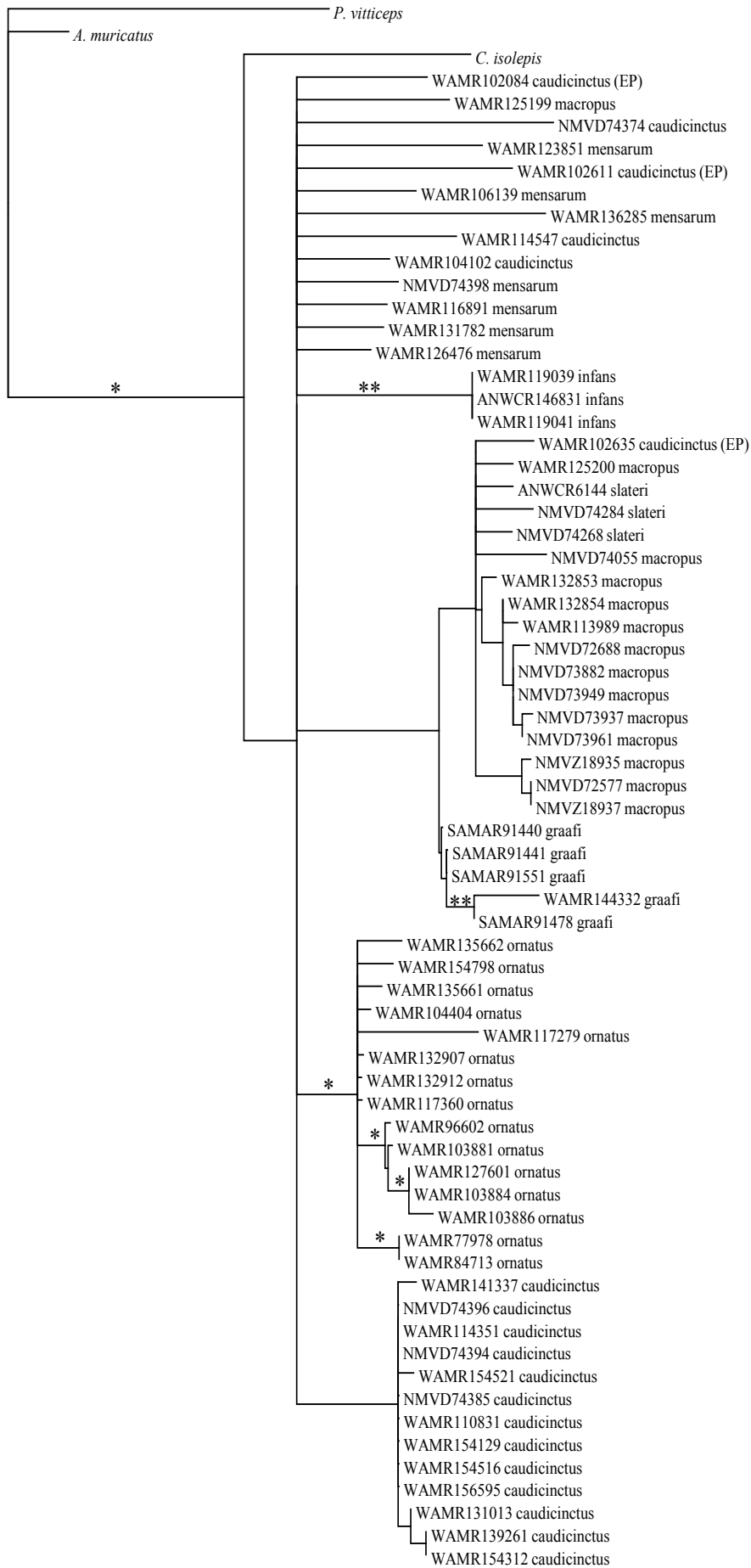NMVD74398 mensarum
WAMR116891 mensarum
WAMR131782 mensarum
WAMR126476 mensarum
WAMR119039 infans
ANWCR146831 infans
WAMR119041 infans
WAMR102635 caudicinctus (EP)
WAMR125200 macropus
ANWCR6144 slateri
NMVD74284 slateri
NMVD74268 slateri
NMVD74055 macropus
WAMR132853 macropus
WAMR132854 macropus
WAMR113989 macropus
NMVD72688 macropus
NMVD73882 macropus
NMVD73949 macropus
NMVD73937 macropus
NMVD73961 macropus
NMVZ18935 macropus
NMVD72577 macropus
NMVZ18937 macropus
SAMAR91440 graafi
SAMAR91441 graafi
SAMAR91551 graafi
WAMR144332 graafi
SAMAR91478 graafi
WAMR135662 ornatus
WAMR154798 ornatus
WAMR135661 ornatus
WAMR104404 ornatus
WAMR117279 ornatus
WAMR132907 ornatus
WAMR132912 ornatus
WAMR117360 ornatus
WAMR96602 ornatus
WAMR103881 ornatus
WAMR127601 ornatus
WAMR103884 ornatus
WAMR103886 ornatus
WAMR77978 ornatus
WAMR84713 ornatus
WAMR141337 caudicinctus
NMVD74396 caudicinctus
WAMR114351 caudicinctus
NMVD74394 caudicinctus
WAMR154521 caudicinctus
NMVD74385 caudicinctus
WAMR110831 caudicinctus
WAMR154129 caudicinctus
WAMR154516 caudicinctus
WAMR156595 caudicinctus
WAMR131013 caudicinctus
WAMR139261 caudicinctus
WAMR154312 caudicinctus

*
**
**
*
*
*
*

0.01

Clade posterior probabilities: *** > 98%; ** 90-97%; * 80-89%.